

# Tandem Solar Cells Based on High-Efficiency c-Si Bottom Cells: Top Cell Requirements for $>30\%$ Efficiency

Thomas P. White, Niraj N. Lal, and Kylie R. Catchpole

**Abstract**—Tandem solar cells based on crystalline silicon present a practical route toward low-cost cells with efficiencies above 30%. Here, we evaluate a dual-junction tandem configuration consisting of a high-efficiency c-Si bottom cell and a thin-film top cell based on low-cost materials. We show that the minimum top cell efficiency required to reach 30% tandem efficiency ranges from 22% for a bandgap of 1.5 eV to 14% for a bandgap of 2 eV. We investigate these limits using a simple model for a four-terminal tandem to identify the material requirements for the top cell in terms of optical absorption, electronic bandgap, carrier transport, and luminescence efficiency. In particular, we show that even relatively low-quality earth-abundant semiconductor materials with luminescence efficiencies of  $10^{-5}$  and diffusion lengths below 100 nm are compatible with tandem cell efficiencies above 30%. Introducing light trapping in the top cell can increase the efficiency beyond 32% and reduce the required diffusion length below 50 nm. This analysis establishes clear research targets for high-bandgap semiconductor materials and novel thin-film solar cell concepts that can be combined with existing c-Si technology. Such tandem approaches could enable the rapid development of a new generation of low-cost high-efficiency cells.

**Index Terms**—Earth-abundant semiconductors, multijunction solar cells, photovoltaics, tandem solar cells, thin-film solar cells.

## I. INTRODUCTION

THE cost of silicon photovoltaics has decreased dramatically in recent years due to higher module efficiencies and reduced material and manufacturing costs. However, single-junction crystalline silicon (c-Si) solar cells are rapidly approaching practical and theoretical efficiency limits. Industrial-scale processes are now capable of producing large-area cells with efficiencies exceeding 24% [1], while the research efficiency record of 25% has stood for almost 15 years [2], [3]. As commercial production approaches these limits, further cost reductions will only be possible through more economical manufacturing unless a practical solution can be found to push efficiencies toward 30% and beyond.

Manuscript received June 17, 2013; revised September 6, 2013; accepted September 19, 2013. Date of publication October 9, 2013; date of current version December 16, 2013. This work was funded by the Australian Renewable Energy Agency and the Australian Research Council.

The authors are with the Centre for Sustainable Energy Systems, Research School of Engineering, Australian National University, Canberra, A.C.T. 0200, Australia (e-mail: thomas.white@anu.edu.au; niraj.lal@anu.edu.au; kylie.catchpole@anu.edu.au).

Color versions of one or more of the figures in this paper are available online at <http://ieeexplore.ieee.org>.

Digital Object Identifier 10.1109/JPHOTOV.2013.2283342

Multijunction solar cells that combine low- and high-bandgap materials tailored to the incident solar spectrum have theoretical efficiencies of 44% for two junctions and up to 65% for an infinite stack of junctions under 1-sun illumination [4]. The additional complexity and cost of fabricating tandem solar cells has so far limited their use in terrestrial applications, but they are likely to become more competitive as single-junction module efficiencies plateau. Tandem cell approaches that exploit existing high-efficiency c-Si technology will benefit directly from recent global investment in c-Si manufacturing.

Despite the dominance of c-Si solar cells, research into their use in tandem modules has been limited. Si top cells combined with low-bandgap Ge bottom cells have been predicted to yield absolute efficiency gains of 2.9% for 1-sun concentration, and 5.8% for 50 suns, compared with an optimized Si cell [5]. Si cells have also been proposed as one of six cells in high-efficiency tandem modules capable of efficiencies above 50% [6]. Tandems based on amorphous and microcrystalline or nanocrystalline Si (sometimes referred to as micromorph cells) have also been widely studied [7]–[9], however, their efficiency is presently only  $\sim 12\%$ . With the exception of micromorph cells, tandem cell development has focused on high electronic quality direct bandgap semiconductors such as the III–V group of compounds [10], [11]. These materials are expensive and have limited abundance to support a global-scale photovoltaic market.

Here, we propose a tandem cell concept that combines low-cost thin-film solar cell technology with existing high-efficiency c-Si cells in a mechanically stacked configuration. In particular, we evaluate top cells that are characterized by strong absorption and poor electronic quality; typical characteristics of new earth-abundant semiconductors being considered as alternative photovoltaic materials. The potential for such materials has been evaluated in terms of abundance and cost [12], and for specific single-junction cell geometries [13], [14], but their application in multijunction cells has not been explored. While significant development is still required to make efficient cells based on these materials, it is important to establish general material and cell performance targets in order to identify the most promising materials and focus the research effort. For this reason, we develop here a simple model to calculate the power conversion efficiency of the tandem cell in terms of bandgap, absorption coefficient, carrier diffusion length, and luminescence efficiency of the top cell. We use this model to evaluate the theoretical efficiency limits for a range of material parameters and determine the requirements to achieve efficiencies in excess of 30%. We

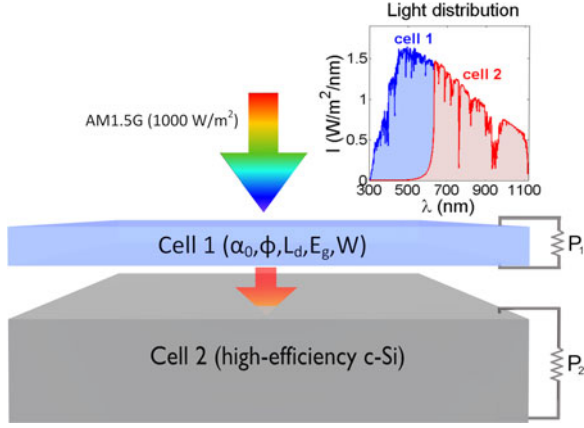


Fig. 1. Schematic of the two-cell tandem configuration considered. Cell 1 (absorber thickness  $W$ ), is made from a direct bandgap semiconductor material, characterized by its bandgap  $E_g$ , absorption coefficient  $\alpha_0$ , carrier diffusion length  $L_d$ , and luminescence efficiency  $\Phi$ . Cell 2 is a high-efficiency c-Si cell with an efficiency of 25% under standard conditions [2]. Inset: distribution of incident energy absorbed in an idealized tandem cell.

also evaluate the benefit of light trapping in the top cell as a function of the material properties.

## II. TANDEM CELL MODEL

Fig. 1 illustrates the tandem cell configuration consisting of a thin top cell (cell 1) of thickness  $W$  and a high-efficiency c-Si bottom cell (cell 2), with independent electrical connections. We consider a four-terminal mechanically stacked tandem as this allows greater flexibility in the choice of bandgap and absorption distribution between the two cells, since current matching is not required. This configuration is also easier to fabricate, especially when combining different material systems.

The maximum power produced by each cell is calculated as the product of short-circuit current  $J_{sc}$ , open-circuit voltage  $V_{oc}$ , and the fill-factor. We choose this macro-approach rather than a more detailed model of the current–voltage response, since the latter requires assumptions about equivalent circuits, recombination mechanisms, and cell resistances. Such an approach loses generality; therefore, here, these additional contributions are included implicitly in the fill-factor.

In the following analysis, we consider 1-sun AM1.5G illumination with incident intensity of  $1000 \text{ W/m}^2$ . We assume no reflectance loss from the cell surfaces and no parasitic optical loss. In this case, the light reaching the bottom cell is simply a function of the top cell’s absorption properties, which are given by the cell thickness and absorption coefficient.

In Section II-A, we first derive an expression for the short-circuit current of the top cell based on the absorbed flux and the collection probability. The open-circuit voltage is derived as a function of the cell’s luminescence efficiency, which sets a maximum achievable voltage based on thermodynamic arguments. Finally, the fill-factor is included as a performance parameter; the effect of which we explore in more detail in Section III-D.

The model for the bottom cell is described in Section II-B, with parameters based on the world-record c-Si PERL cell [2], [3]. The generated photocurrent is calculated from the photon

flux transmitted through the top cell, including an effective collection probability based on the short-circuit current at standard test conditions. The resulting decrease in voltage from the bottom cell is taken into account via the diode equation. The bottom cell fill factor is treated as a constant, independent of  $J_{sc}$  and  $V_{oc}$ .

### A. Top Cell

Cell 1 is modeled as a p-i-n heterojunction cell with a thin intrinsic absorbing layer sandwiched between transparent hole and electron conducting layers. This is the most versatile cell geometry for thin-film absorbers as it does not require doping of the absorber layer and it offers higher carrier collection efficiencies than equivalent cells with a p-n junction [15].

The absorbing layer is modeled as a direct bandgap semiconductor with bandgap  $E_g$ , and absorption coefficient  $\alpha$  given by the analytic approximation

$$\alpha(\lambda) = \alpha_0 \left( \frac{E_\varphi(\lambda) - E_g}{kT} \right)^{1/2} \quad (1)$$

where  $\alpha_0$  is the characteristic absorption coefficient for the material,  $E_\varphi(\lambda) = hc/\lambda$  is the incident photon energy at wavelength  $\lambda$ ,  $k$  is the Boltzmann constant, and  $T = 298 \text{ K}$  is the cell temperature.

We consider two cases for light absorption in the top cell. The first case is single-pass absorption, given by  $A^{(1)} = 1 - \exp(-\alpha W)$ , where the superscript (1) refers to the top cell. In the second case, we consider the conventional light trapping limit for Lambertian scattering in the top cell [16]

$$A^{(1)} = \frac{1 - \exp(-2\alpha W_{op})}{1 - (1 - 1/n^2) \exp(-2\alpha W_{op})} \quad (2)$$

where  $W_{op} = W \frac{2+a(\alpha W)^b}{1+a(\alpha W)^b}$ ,  $a = 0.935$  and  $b = 0.67$ .

While this limit is strictly valid only when  $W \gg \lambda$ , it still provides a useful benchmark for thin absorbers, where light trapping can exceed the conventional limits [17]. Equation (2) holds when the back surface of the cell is an ideal reflector of above-bandgap photons. This could be achieved in a tandem cell using a wavelength-selective Bragg mirror between the top and bottom cells. We also assume that all nonabsorbed light is transmitted to the bottom cell. We use  $n = 3$  in (2) as a typical refractive index for a semiconductor absorbing layer and note that the results depend weakly on this choice when  $2.5 < n < 3.5$ . The light transmitted through the top cell and incident on the bottom cell is given by  $T^{(1)} = 1 - A^{(1)}$ .

The electrical properties of the top cell are characterized by the carrier diffusion length  $L_d$ , luminescence efficiency  $\Phi$ , and the cell fill factor  $FF^{(1)}$ . The carrier diffusion length is taken to be equal for holes and electrons. The short-circuit current is determined by the absorption of incident light and carrier collection probability  $f_c$

$$J_{sc}^{(1)} = f_c q \int_0^\infty \phi_{AM1.5G}(\lambda) A^{(1)}(\lambda) d\lambda \quad (3)$$

where  $\phi_{AM1.5G}(\lambda)$  is the incident photon flux, and  $q$  is the electron charge. Carrier collection in a p-i-n cell is assisted by

the built-in voltage,  $V_{bi}$  across the intrinsic absorbing layer, and can be calculated using the analytic expressions provided in [15] and [18]

$$f_c = \frac{\exp(\lambda_2^0/2) - 1}{\lambda_2^0/2} \quad (4)$$

where

$$\lambda_2^0 = \frac{qV_{bi}}{2kT} - \sqrt{\left(\frac{W}{L_d}\right)^2 + \left(\frac{qV_{bi}}{2kT}\right)^2}. \quad (5)$$

Following [18], we make the approximation  $V_{bi} = E_g$ . Evaluation of (4) and (5) shows that efficient carrier collection is possible in thin absorbers, even when the  $W > L_d$  [15]. In practice, the collection efficiency may be reduced by the presence of defects and grain boundaries in the absorbing layer, but these contributions are not considered here.

The maximum top cell voltage depends on the absorber bandgap and carrier recombination. Here, we characterize recombination by a single parameter, the photoluminescence efficiency  $\Phi$ , defined as the ratio of radiative recombination to total recombination. The radiative properties of a solar cell are closely related to its electrical performance and the radiative efficiency of the absorbing layer provides an estimate of the maximum open-circuit voltage  $V_{oc}$ . We use the relationship derived in [19] to calculate  $V_{oc}$  of the top cell as a function of  $\Phi$  and the absorption properties of the thin film

$$V_{oc}^{(1)} \approx \frac{kT}{q} \ln \left( \frac{J_{sc}^{(1)}}{J_0^{(1)}} \right) + \frac{kT}{q} \ln(\Phi) \quad (6)$$

where

$$J_0^{(1)} = \frac{2\pi n^2}{h^3 c^2} \int_0^\infty \frac{A^{(1)}(E_\varphi) E_\varphi^2}{\exp(E_\varphi/kT) - 1} dE_\varphi \quad (7)$$

is the background blackbody flux at ambient temperature [19]. The first term in (6) is the same as that derived by Shockley and Queisser [20] in the thermodynamic limit, while the second term provides a correction for nonunity photoluminescence efficiency.

We note that the diffusion length and the luminescence efficiency are related via carrier lifetime and mobility. To include this relationship explicitly in the model would require additional assumptions about specific material properties. Hence, we instead treat  $L_d$  and  $\Phi$  as independent parameters that can be experimentally determined to assess the potential of new photovoltaic materials.

Equations (1)–(7) are used to calculate the short-circuit current and open-circuit voltage for the top cell as a function of  $W, E_g, \alpha_0, L_d$ , and  $\Phi$ . The maximum output power per unit area from the top cell is then given by

$$P^{(1)} = P^{(1)}(W, E_g, \alpha_0, L_d, \Phi) = J_{sc}^{(1)} \times V_{oc}^{(1)} \times FF^{(1)}. \quad (8)$$

The fill-factor,  $FF^{(1)}$ , is treated as a cell performance parameter, the impact of which is discussed in Section III-D.

## B. Bottom Cell

The bottom cell of the tandem is modeled on the 25% efficient c-Si PERL cell reported in [2], with revised performance parameters  $V_{oc} = 0.706$  V,  $J_{sc} = 42.7$  mA/cm<sup>2</sup>, and  $FF = 82.8\%$  under standard test conditions [3]. In the tandem configuration, cell 2 only receives light that is transmitted through cell 1; therefore,  $V_{oc}^{(2)}$  and  $J_{sc}^{(2)}$  must be modified accordingly. We assume that the fill factor does not change significantly, and therefore use a fixed value of  $FF^{(2)} = 82.8\%$  for the following calculations.

To estimate the short-circuit current in cell 2 under nonstandard illumination, we first calculate the photocurrent generated in a 400- $\mu$ m c-Si wafer with Lambertian light trapping and no reflection loss under AM1.5G illumination (43.7 mA/cm<sup>2</sup>), and compare this with the measured value to derive an effective collection probability of 0.978. The short-circuit current from cell 2 is then evaluated using

$$J_{sc}^{(2)} = 0.978q \int \phi_{AM1.5G}(\lambda) T^{(1)}(\lambda) A^{(2)}(\lambda) d\lambda \quad (9)$$

where  $\phi_{AM1.5G}(\lambda) T^{(1)}(\lambda)$  is the photon flux transmitted through cell 1.  $A^{(2)}(\lambda)$  is calculated using an equivalent expression to (2), but with the optical properties of c-Si [21] and an absorber thickness of 400  $\mu$ m. Equation (9) does not include the wavelength dependence of the internal quantum efficiency, but it is sufficiently accurate for the purposes of this study.

The open-circuit voltage is calculated from the current in (9) using the diode equation

$$V_{oc}^{(2)} = \frac{kT}{q} \ln \left( \frac{J_{sc}^{(2)}}{J_0^{(2)}} + 1 \right) \quad (10)$$

where  $J_0^{(2)} = 4.9 \times 10^{-11}$  A/cm<sup>2</sup> gives the reported performance under standard illumination. We can therefore calculate the power from cell 2 as a function of the absorption properties of cell 1 using (9) and (10)

$$P^{(2)} = P^{(2)}(W, E_g, \alpha_0) = J_{sc}^{(2)} \times V_{oc}^{(2)} \times FF^{(2)}. \quad (11)$$

Finally, assuming lossless power addition, the overall efficiency of the tandem configuration in Fig. 1 is

$$\eta = \frac{P^{(1)}(W, E_g, \alpha_0, L_d, \Phi) + P^{(2)}(W, E_g, \alpha_0)}{1000 \text{ W/m}^2}. \quad (12)$$

## III. RESULTS

The model that is described in Section II provides an efficient way to identify performance requirements for a thin-film top cell in tandem with a high-efficiency silicon bottom cell. In this section, we first calculate the minimum efficiency requirements for a top cell based only on the reduced current and voltage in the bottom cell (see Section III-A). This provides very clear targets for top cell development. Then, in Sections III-B and III-D, we consider in more detail the top cell properties that would allow these efficiency targets to be reached. We evaluate the conversion efficiency of the two-junction tandem cell as a function of bandgap, luminescence efficiency, diffusion length, absorption, and fill factor of the top cell. For each combination

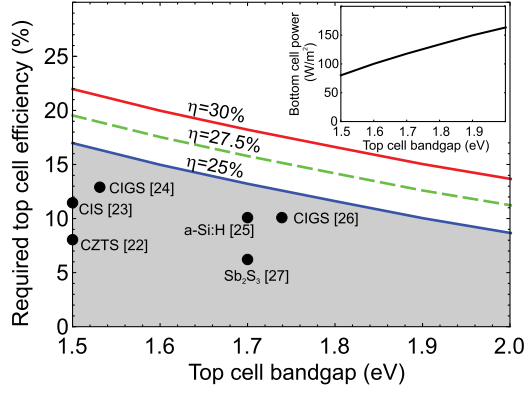


Fig. 2. Top cell conversion efficiency required for a c-Si based tandem cell to reach a conversion efficiency of  $\eta = 25\%$  (blue solid curve),  $27.5\%$  (green-dashed curve), and  $30\%$  (red solid curve). The shaded area indicates areas where  $\eta < 25\%$ . Dots indicate experimental cell efficiencies reported for several high-bandgap materials. Inset: output power of the bottom cell when the top cell absorbs all photons with energy above the bandgap.

of these parameters, we optimize the top cell thickness  $W$  to maximize the tandem cell efficiency.<sup>1</sup>

The choice of material properties is intended to cover a wide range of possible top cell materials, with a particular focus on earth-abundant inorganic semiconductors [12]. For this reason, we consider materials with relatively strong absorption coefficients ( $\alpha_0 = 10^4 \text{ cm}^{-1}$ ) and short diffusion lengths ( $L_d < 200 \text{ nm}$ ), which are representative of many such materials.

The results in Sections III-B and III-C are calculated for a top cell fill factor  $FF^{(1)} = 0.8$ . This is chosen as a practical future performance target, and is higher than the reported experimental results for most novel earth-abundant material systems. The value is consistent with the upper limits for single-junction cells based on thermodynamic and semiempirical arguments [7]. The dependence on fill factor is studied in Section III-D.

#### A. Minimum Efficiency Requirements for the Top Cell

The top cell in a tandem is illuminated by the full solar photon flux, therefore, the power it produces is related directly to its conversion efficiency under standard test conditions. The bottom cell receives a filtered photon flux and produces a correspondingly lower power than it would under AM1.5G illumination. Thus, for the tandem cell to reach an overall conversion efficiency of  $30\%$  ( $300 \text{ W/m}^2$  output under standard test conditions), the top cell must compensate for the reduced power in the c-Si bottom cell, and produce an extra  $50 \text{ W/m}^2$ .

It is straightforward to estimate the efficiency requirements of the top cell by considering the power produced by the bottom cell. If the top cell absorbs all incident photons with energy above its bandgap  $E_g$ , we can evaluate (9) by setting  $T^{(1)}(\lambda) = 0$  for  $\lambda < hc/E_g$ , and  $T^{(1)}(\lambda) = 1$  otherwise.  $P^{(2)}$  can then be calculated from (10) and (11). The inset in Fig. 2 shows the bottom cell power as a function of the top cell bandgap in this case. When  $E_g$  is large, the top cell only absorbs a small

<sup>1</sup>For some combinations of top cell parameters,  $V_{oc}^{(1)} < V_{oc}^{(2)}$  for all  $W$ . In this case, the top cell provides no benefit, and the maximum efficiency is  $\eta = 25\%$  when  $W = 0$ .

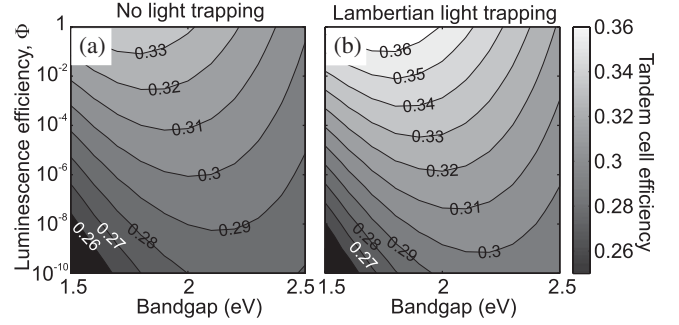


Fig. 3. Total efficiency of the tandem cell configuration shown in Fig. 1, calculated as a function of the bandgap and luminescence efficiency of cell 1. (a) Single-pass absorption. (b) Lambertian light trapping. Results were calculated with  $\alpha_0 = 1 \times 10^4 \text{ cm}^{-1}$  and  $L_d = 100 \text{ nm}$ .

fraction of the incident photons, and the bottom cell produces the maximum power. As  $E_g$  decreases toward the bandgap of the bottom cell, fewer photons reach the bottom cell and the power decreases.

The main axis in Fig. 2 shows the top cell efficiency required for tandem cell efficiencies of  $\eta = 25\%$ ,  $27.5\%$ , and  $30\%$ . The curves are calculated from the difference between the desired output power and the bottom cell power. These results illustrate the need for a relatively high-efficiency top cell. For example, if  $E_g = 1.5 \text{ eV}$ , a top cell efficiency of  $17\%$  is required just to recover the power lost from the bottom cell, and a  $22\%$  efficient top cell would be needed to achieve a tandem efficiency of  $\eta = 30\%$ . The top cell efficiency reduces as  $E_g$  increases, but at the same time the absorbed photon flux decreases. For  $E_g = 2 \text{ eV}$ , a  $9\%$  efficient top cell would yield  $\eta = 25\%$ , and a  $14\%$  efficient top cell would yield  $\eta = 30\%$ .

Fig. 2 also shows the highest experimental cell efficiencies reported in the literature for several high-bandgap semiconductors. At present, none of these has reached a high enough conversion efficiency to compensate the power loss in the bottom cell. We can see, however, that the  $\text{Cu(In,Ga)S}_2$  (CIGS) compound semiconductors appear to be the most promising of those developed to date. There may be alternative high-bandgap semiconductors that are less well developed, but that also have potential in tandem cells. The analysis in the following sections helps identify specific material requirements that such materials would have to meet in order to achieve the required efficiency. We compare several of the materials shown in Fig. 2 in more detail in Section IV.

#### B. Dependence on Bandgap and Luminescence Efficiency

Following from Section IIIA, we next consider the specific properties required by a top cell to reach conversion efficiencies above  $30\%$ . Fig. 3 shows the maximum efficiency of the tandem stack as a function of the bandgap and luminescence efficiency for  $\alpha_0 = 10^4 \text{ cm}^{-1}$ , and  $L_d = 100 \text{ nm}$ . These plots illustrate a number of important results. First, it can be seen that light trapping provides significant benefits for this combination of  $\alpha_0$  and  $L_d$ , offering absolute efficiency increases of up to  $3\%$  for materials with high luminescent efficiency. Second, the optimum top cell bandgap increases as the luminescence

efficiency decreases. In the limit of pure radiative recombination,  $\Phi = 1$ , the optimum bandgap is  $E_g \sim 1.7$  eV, which is consistent with ultimate efficiency limits derived for two-junction tandem cells [4], [7]. In this case, the optimum bandgap is the same for series-connected and four-terminal tandems. As nonradiative recombination increases, the optimum bandgap increases. This can be understood from (6): as  $\Phi$  decreases, the voltage drop due to nonradiative recombination increases, and thus, the voltage benefit provided by the top cell is reduced. Increasing the top cell bandgap can partially compensate this voltage drop, but at the expense of current, and thus, the optimum bandgap increases gradually from  $E_g \sim 1.7$  eV at  $\Phi = 1$  to  $E_g \sim 2.25$  eV at  $\Phi = 10^{-10}$ . Similar trends were recently identified for multijunction series-connected cells in [28].

Fig. 3 shows the total efficiency calculated for a wide range of luminescence efficiencies, and clearly illustrates the strong dependence of efficiency limits on recombination in the top cell. While photoluminescence and electroluminescence are both widely used to characterize solar cells, absolute values of  $\Phi$  are rarely reported in the literature. We can, however, use (6) to infer lower limits for  $\Phi$  based on experimental  $V_{oc}$  values reported for different PV materials. For example, high-performance GaAs ( $E_g \sim 1.4$  eV) cells have been reported with  $V_{oc} = 1.12$  V [29], indicating  $\Phi > 0.5$ . Similarly, high-efficiency c-Si ( $E_g \sim 1.12$  eV) cells achieve  $V_{oc} > 0.7$  V, corresponding to  $\Phi > 10^{-3}$ . More relevant to this study is amorphous Si ( $E_g \sim 1.6$  eV), which is representative of a well-studied and optimized semiconductor with relatively poor electronic quality. Open-circuit voltages as high as 1.04 V have been reported for a-Si cells [30], corresponding to  $\Phi \sim 10^{-5}$ . Similar luminescent efficiency values were calculated by Green in a recent analysis of experimental cell performance [31].

Considering a material with  $\Phi = 10^{-5}$ , Fig. 3 shows an optimum  $E_g \sim 1.95$  eV for which the maximum efficiency is  $\eta = 30.6\%$  for the single-pass absorption case and 32.6% with light trapping. The optimum absorber thicknesses are 464 and 166 nm, respectively. Fig. 3 also shows that the total power output is a relatively weak function of the top cell bandgap. Considering  $\Phi = 10^{-5}$  again, efficiencies  $>30\%$  are predicted for  $1.5 < E_g < 2.5$  eV with light trapping. This provides significant flexibility in the choice of top cell absorber material, and is another major advantage of the four-port tandem compared with series-connected cells.

### C. Dependence on Diffusion Length and Luminescence Efficiency

We next consider the influence of carrier diffusion length in the top cell. Fig. 4 shows the maximum efficiency as a function of  $L_d$  and  $\Phi$  for  $\alpha_0 = 1 \times 10^4$  cm $^{-1}$  (as in Fig. 3), and  $E_g = 1.95$  eV, corresponding to the optimum bandgap for  $\Phi = 10^{-5}$ . Not surprisingly, in both Fig. 4(a) and (b) the efficiency increases with diffusion length as a result of improved collection efficiency. In the light-trapping case [see Fig. 4(b)], however, there is little increase in efficiency once  $L_d > 100$  nm, indicating that for this combination of  $\alpha_0$  and  $E_g$ , the absorption and collection efficiencies are almost unity. For the single-pass

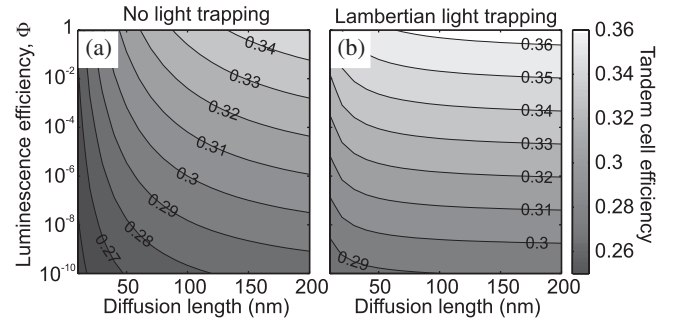


Fig. 4. Total efficiency of the tandem cell configuration shown in Fig. 1, calculated as a function of the diffusion length and luminescence efficiency of cell 1. (a) Single-pass absorption. (b) Lambertian light trapping. Results were calculated with  $\alpha_0 = 1 \times 10^4$  cm $^{-1}$  and  $E_g = 1.95$  eV.

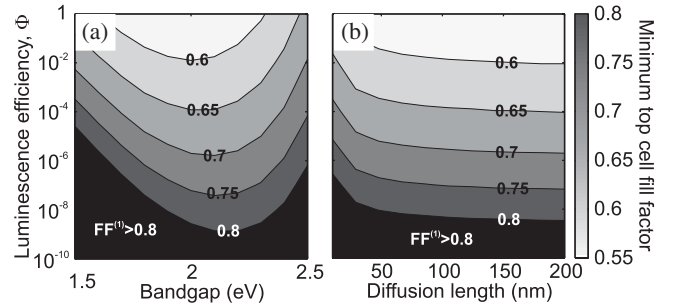


Fig. 5. Minimum top cell fill factor required for 30% conversion efficiency in the tandem cell with light trapping in the top cell. (a) Minimum FF as a function of the top cell bandgap and luminescence efficiency when  $L_d = 100$  nm. (b) Minimum FF as a function of top cell diffusion length and luminescence efficiency when  $E_g = 1.95$  eV. Results were calculated with  $\alpha_0 = 1 \times 10^4$  cm $^{-1}$ .

absorption case [see Fig. 4 (a)], increasing the diffusion length beyond 200 nm would still provide significant benefit.

Fig. 4(b) also shows the significant benefit of light trapping for materials with very poor luminescence efficiency and short diffusion lengths. For example, efficiencies of 30% can still be achieved for  $\Phi = 10^{-8}$  and  $L_d = 35$  nm, despite the low value of  $\Phi$  limiting the top cell  $qV_{oc}$  to only  $0.6 E_g$ .

### D. Dependence on Top Cell Fill Factor

Finally, we consider the importance of the top cell fill-factor on the overall tandem cell efficiency. The results in Section III-B and III-C were calculated for  $FF^{(1)} = 0.8$  which is a relatively ambitious performance target for a novel thin-film cell. To set research targets for the fill factor, we evaluate the minimum top cell fill factor required to reach an efficiency of 30% with light trapping in the top cell. The results are shown in Fig. 5, calculated for the same parameter space as Figs. 3(b) and 4(b), respectively. The results show that  $FF^{(1)} = 0.8$  is not required unless the luminescence efficiency is very low. Considering the previous example of a top cell with  $\Phi = 10^{-5}$ ,  $E_g = 1.95$  eV, and  $L_d = 100$  nm, we find the minimum fill factor is  $FF^{(1)} = 0.69$  to achieve 30% efficiency. Lower fill factors would require a higher luminescence efficiency (corresponding to higher  $V_{oc}$ ). For example, if  $FF^{(1)} = 0.6$ , a minimum  $\Phi = 10^{-2}$  is required to pass 30% conversion efficiency.

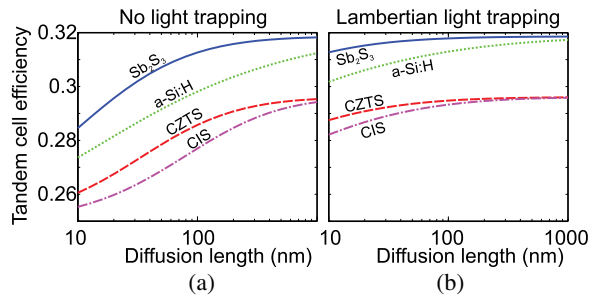


Fig. 6. Comparison of maximum tandem cell efficiencies for different top cell absorber materials assuming a top cell fill factor  $FF^{(1)} = 0.8$ , and luminescence efficiency  $\Phi = 10^{-5}$ . (a) Single-pass absorption (b) Lambertian light trapping.

#### IV. DISCUSSION

The results in Section III provide specific targets for material and cell development in order to reach tandem efficiencies of 30% and higher. While the calculations neglect optical loss and explicit surface recombination, they provide upper estimates of achievable efficiencies. The results can thus be used to quickly assess the potential of new and existing semiconductor materials for this application. As an example, here, we select four possible top cell absorber materials that have already shown promise in single-junction cells and assess their suitability for a tandem cell with c-Si.

The four materials we consider are CuInS<sub>2</sub> (CIS), Cu<sub>2</sub>ZnSnS<sub>4</sub> (CZTS), amorphous silicon (a-Si:H), and Sb<sub>2</sub>S<sub>3</sub>. CIS and CZTS are both chalcopyrite materials with a bandgap of  $E_g \sim 1.5$  eV, which is at the lower end of the range in Figs. 3–6. They have absorption coefficients on the order of  $10^4$ – $10^5$  cm<sup>-1</sup>. CIS cells have reached efficiencies of 11.4% [23], and up to 12.9% with the addition of gallium [24]. CZTS has been proposed as an earth-abundant alternative to Cu(In,Ga)(S,Se) (CIGS) cells, with efficiencies of up to 8.4% demonstrated to date [22]. Of the other two materials, a-Si:H has  $E_g \sim 1.6$ – $1.7$  eV, and Sb<sub>2</sub>S<sub>3</sub> has  $E_g \sim 1.7$  eV, and thus they are closer to the optimum top cell bandgap. Sb<sub>2</sub>S<sub>3</sub> has the largest absorption coefficient of the four materials; almost twice as large as that of CZTS [32]–[35]. The record efficiency for an a-Si:H cell is 10.1% [25], while Sb<sub>2</sub>S<sub>3</sub> has been used as an absorber in nanostructured solar cells with efficiencies up to 6% [27], [36].

To include the real absorption properties of these materials in the model, we replace the analytic expression for  $\alpha(\lambda)$  in (1) with experimental values from the literature [32]–[35] for all above bandgap wavelengths, and set  $\alpha = 0$  for sub-bandgap light. Fig. 6 shows the calculated tandem cell efficiencies for each material as a function of  $L_d$ . For comparison, the results were all calculated for  $\Phi = 10^{-5}$ ,  $FF^{(1)} = 0.8$ , and optimal cell thickness, and thus, the efficiency differences between the materials are due to their bandgaps and optical absorption characteristics. As expected, Fig. 6 shows that in the limit of unity collection efficiency (large  $L_d$  and/or large  $\alpha$ ), the efficiency is determined by the top cell bandgap. Thus, for the examples considered here, the limiting efficiency for a tandem with a CIS or CZTS top cell is 29.5%, while for a-Si:H and Sb<sub>2</sub>S<sub>3</sub> the maximum efficiency is 31.8%. The benefits of strong absorption are also clear, particularly

in Fig. 6(a) where there is no light trapping. In this case, a diffusion length of 30 nm would be sufficient to achieve 30% efficiency with a Sb<sub>2</sub>S<sub>3</sub> top cell, whereas a diffusion length of 125 nm and a considerably thicker cell would be required for the same efficiency using a-Si:H as the absorber. In fact, the electron diffusion length in Sb<sub>2</sub>S<sub>3</sub> films is estimated to be 33 nm in [37], indicating that it may be a good candidate for further development. The reported diffusion lengths for CZTS and CIS are considerably larger ( $\sim 350$  nm for CZTS [22] and  $\sim 1$   $\mu$ m for CIS [38]), but their suitability for tandem applications with c-Si is limited given the limit on the efficiency due to the smaller bandgap. Cu(In,Ga)S<sub>2</sub> based cells, two of which are shown in Fig. 2, may be more promising, as the In/Ga ratio can be varied to tune the bandgap up to 1.8 eV [26]. However, the long-term use of relatively rare elements such as In and Ga in photovoltaics is uncertain.

It is also important to note that of the four materials that are considered in this section, only a-Si:H and CIS cells have so far achieved open-circuit voltages higher than the best c-Si cells. Since this is an essential requirement for a top cell in any tandem configuration, it clearly indicates the need for further material and cell development before the c-Si based tandem concept becomes viable. Nevertheless, our simple model provides a rapid means of identifying the most promising materials on which to focus research efforts.

#### V. CONCLUSION

These results demonstrate the potential for tandem cells that combine existing high-efficiency c-Si technology with low-cost cells based on strongly-absorbing earth-abundant semiconductors. We have studied systematically the influence of the top cell's bandgap, absorption coefficient, diffusion length, and luminescence efficiency on tandem cell efficiencies. In particular, our results show that efficiencies greater than 30% are possible using thin-film absorbers in the top cell with carrier diffusion lengths on the order of 100 nm and luminescence efficiencies of  $10^{-5}$ . Reaching these efficiencies with low-quality semiconductors requires a top cell bandgap approaching 2 eV to compensate for the voltage loss due to recombination. This is likely to provide a significant advantage to four-port tandem configurations compared with series-connected modules, since current matching is not required, and thus, choice of bandgaps is more flexible.

#### REFERENCES

- [1] P. J. Cousins, D. D. Smith, H-C. Luan, J. Manning, T. D. Dennis, A. Waldhauer, K. A. Wilson, G. Hartley, and W. P. Mulligan, "Generation 3: Improved performance at lower cost," in *Proc. 33rd IEEE Photovoltaic Spec. Conf.*, 2010, pp. 275–278.
- [2] Z. Zhao, A. Wang, M. A. Green, and F. Ferrazza, "19.8% efficient "honeycomb" textured multicrystalline and 24.4% monocrystalline silicon solar cells," *Appl. Phys. Lett.*, vol. 73, no. 14, pp. 1991–1993, 1998.
- [3] M. A. Green, "The path to 25% silicon solar cells efficiency: History of the silicon cell evolution," *Prog. Photovoltaics: Res. Appl.*, vol. 17, pp. 183–189, 2009.
- [4] A. Martí and G. L. Araújo, "Limiting efficiencies for photovoltaic energy conversion in multigap systems," *Sol. Energy Mater. Sol. Cells*, vol. 43, pp. 203–222, 1996.

- [5] C. Kerestes, Y. Wang, K. Shreve, J. Mutitu, T. Creazzo, P. Murcia, and A. Barnett, "Design, fabrication, and analysis of transparent silicon solar cells for multi-junction assemblies," *Prog. Photovoltaics: Res. Appl.*, vol. 21, pp. 578–587, 2013.
- [6] A. Barnett, D. Kirkpatrick, C. Honsberg, D. Moore, M. Wanlass, K. Emery, R. Schwartz, D. Carlson, S. Bowden, D. Aiken, A. Gray, S. Kurtz, L. Kazmerski, M. Steiner, J. Gray, T. Davenport, R. Buelow, L. Takacs, N. Shatz, J. Bortz, O. Jani, K. Goossen, F. Kiamilev, A. Doolittle, I. Ferguson, B. Unger, G. Schmidt, E. Christensen, and D. Salzman, "Very high efficiency solar cell modules," *Prog. Photovoltaics: Res. Appl.*, vol. 17, pp. 75–83, 2009.
- [7] F. Meillaud, A. Shah, C. Droz, E. Vallat-Sauvain, and C. Miazza, "Efficiency limits for single-junction and tandem solar cells," *Sol. Energy Mater. Sol. Cells*, vol. 90, pp. 2952–2959, 2006.
- [8] H. Keppner, J. Meier, P. Torres, D. Fischer, and A. Shah, "Microcrystalline silicon and micromorph tandem solar cells," *Appl. Phys. A*, vol. 69, pp. 169–177, 1999.
- [9] J. Bailat, L. Fresquet, J.-B. Orhan, Y. Djeridane, B. Wolf, P. Madliger, J. Steinhauser, S. Benagli, D. Borello, L. Castens, G. Monteduro, M. Marmelo, B. Dehbozorgi, E. Vallat-Sauvain, X. Multone, D. Romang, J.-F. Boucher, J. Meier, U. Kroll, M. Despeisse, G. bugnon, C. Ballif, S. Marjanivoc, G. Kohnke, N. Borelli, K. Koch, J. Liu, R. Modavis, D. Thelen, S. Vallon, A. Zakharian, and D. Weidman, "Recent developments of high-efficiency micromorph<sup>®</sup> tandem solar cells in Kai-M PECVD reactors," in *Proc. 25th Eur. Photovoltaic Solar Energy Conf. 15th World Conf. Photovoltaic Energy Convers.*, 2010, pp. 2720–2723.
- [10] H. Cotal, C. Fetzer, J. Boisvert, G. Kinsey, R. King, P. Hebert, H. Yoon, and N. Karam, "III-V multijunction solar cells for concentrating photovoltaics," *Energy Environ. Sci.*, vol. 2, pp. 174–192, 2009.
- [11] K. Tanabe, "A review of ultrahigh efficiency III-V semiconductor compound solar cells: Multijunction tandem, lower dimensional, photonic up/down conversion and plasmonic nanometallic structures," *Energies*, vol. 2, pp. 504–530, 2009.
- [12] C. Wadia, A. P. Alivasatos, and D. M. Kammen, "Materials availability expands the opportunity for large-scale photovoltaics deployment," *Environ. Sci. Technol.*, vol. 43, pp. 2072–2077, 2009.
- [13] T. Ditttrich, A. Balaidi, and A. Ennaoui, "Concepts of inorganic solid-state nanostructured solar cells," *Sol. Energy Mater. Sol. Cells*, vol. 95, pp. 1527–1536, 2011.
- [14] D. Hodes and D. Cahen, "All-solid-state semiconductor-sensitized nanoporous solar cells," *Acc. Chem. Res.*, vol. 45, no. 5, pp. 705–713, 2012.
- [15] K. Taretto, U. Rau, and J. H. Werner, "Closed-form expression for the current/voltage characteristics of pin solar cells," *Appl. Phys. A*, vol. 77, pp. 865–871, 2003.
- [16] M. A. Green, "Lambertian light trapping in textured solar cells and light-emitting diodes: Analytical solutions," *Prog. Photovoltaics: Res. Appl.*, vol. 10, pp. 235–241, 2002.
- [17] Z. Yu, A. Raman, and S. Fan, "Fundamental limit of nanophotonic light trapping in solar cells," *Proc. Nat. Acad. Sci. U.S.A.*, vol. 107, pp. 17491–17496, 2010.
- [18] K. Taretto and U. Rau, "Modeling extremely thin absorber solar cells for optimized design," *Prog. Photovoltaics: Res. Appl.*, vol. 12, pp. 573–591, 2004.
- [19] G. Smestad and H. Ries, "Luminescence and current-voltage characteristics of solar cells and optoelectronic devices," *Sol. Energy Mater. Sol. Cells*, vol. 25, pp. 51–71, 1992.
- [20] W. Shockley and H. J. Queisser, "Detailed balance limit of efficiency of pn junction solar cells," *J. Appl. Phys.*, vol. 32, pp. 510–519, 1961.
- [21] M. A. Green and M. J. Keevers, "Optical properties of intrinsic silicon at 300 K," *Prog. Photovoltaics: Res. Appl.*, vol. 3, pp. 189–192, 1995.
- [22] B. Shin, O. Gunawan, Y. Zhu, N. A. Bojarczuk, S. J. Chey, and S. Guha, "Thin film solar cell with 8.4% power conversion efficiency using and earth-abundant  $\text{Cu}_2\text{ZnSnS}_4$  absorber," *Prog. Photovoltaics: Res. Appl.*, vol. 21, pp. 72–76, 2013.
- [23] K. Siemer, J. Klaer, I. Luck, J. Bruns, R. Klenk, and D. Bräunig, "Efficient  $\text{CuInS}_2$  solar cells from a rapid thermal process (RTP)," *Sol. Energy Mater. Sol. Cells*, vol. 67, pp. 159–166, 2001.
- [24] S. Merdes, D. Abou-Ras, R. Mainz, R. Klenk, M. Ch. Lux-Steiner, A. Meeder, H. W. Schock, and J. Klaer, "CdS/Cu(In,Ga)S<sub>2</sub> based solar cells with efficiencies reaching 12.9% prepared by a rapid thermal process," *Prog. Photovoltaics: Res. Appl.*, vol. 21, pp. 88–93, 2013.
- [25] S. Benagli, D. Borello, E. Vallat-Sauvain, J. Meier, U. Kroll, J. Hoetzal, J. Bailat, J. Steinhauser, M. Marmelo, G. Monteduro, and L. Castens, "High-efficiency amorphous silicon devices on LPCVD-ZNO TCO prepared in industrial KAI-M R&D reactor," in *Proc. 24th Eur. Photovoltaic Sol. Energy Conf. 15th World Conf. Photovoltaic Energy Convers.*, 2009, pp. 2293–2298.
- [26] R. Kaigawa, A. Neisser, R. Klenk, and M. Ch. Lux-Steiner, "Improved performance of thin film solar cells based on  $\text{Cu}(\text{In,Ga})\text{S}_2$ ," *Thin Solid Films*, vol. 415, pp. 266–271, 2002.
- [27] S. H. Im, C.-S. Lim, J. A. Chang, Y. H. Lee, N. Maiti, H.-J. Kim, Md. K. Nazeeruddin, M. Grätzel, and S. I. Seok, "Toward interaction of sensitizer and functional moieties in hole-transporting materials for efficient semiconductor-sensitized solar cells," *Nano Lett.*, vol. 11, pp. 4789–4793, 2011.
- [28] N. L. A. Chan, N. J. Ekins-Daukes, J. G. J. Adams, M. P. Lumb, M. Gonzalez, P. P. Jenkins, I. Vurgaftman, J. R. Meyer, and R. J. Walters, "Optimal bandgap combinations—Does material quality matter?," *IEEE J. Photovoltaics*, vol. 2, no. 2, pp. 202–208, Apr. 2012.
- [29] M. A. Green, K. Emery, Y. Hishikawa, W. Warta, and E. D. Dunlop, "Solar cell efficiency tables (version 41)," *Prog. Photovoltaics: Res. Appl.*, vol. 21, pp. 1–11, 2013.
- [30] X. Deng, K. L. Narasimhan, J. Evans, M. Izu, and S. R. Ovshinsky, "Dependence of a-Si solar cell  $V_{oc}$  on deposition temperature," in *Proc. IEEE Photovoltaic Spec. Conf.*, 1994, vol. 1, pp. 678–681.
- [31] M. Green, "Radiative efficiency of state-of-the-art photovoltaic cells," *Prog. Photovoltaics: Res. Appl.*, vol. 20, pp. 472–476, 2012.
- [32] C. Ghosh and B. P. Varma, "Optical properties of amorphous and crystalline  $\text{Sb}_2\text{S}_3$  thin films," *Thin Solid Films*, vol. 60, pp. 61–65, 1979.
- [33] J. Li, H. Du, J. Yarbrough, A. Norman, K. Jones, G. Teeter, F. L. Terry Jr., and D. Levi, "Spectral optical properties of  $\text{Cu}_2\text{ZnSnS}_4$  thin film between 0.73 and 6.5 eV," *Opt. Express*, vol. 20, no. S2, pp. A327–A332, 2012.
- [34] C. Guillén, "CuInS<sub>2</sub> thin films grown sequentially from binary sulfides as compared to layers evaporated directly from the elements," *Semicond. Sci. Technol.*, vol. 21, pp. 709–712, 2006.
- [35] O. Vetterl, F. Finger, R. Carius, P. Hapke, L. Houben, O. Kluth, A. Lambert, A. Mück, B. Rech, and H. Wagner, "Intrinsic microcrystalline silicon: A new material for photovoltaics," *Sol. Energy Mater. Sol. Cells*, vol. 62, pp. 97–108, 2000.
- [36] S. Ito, K. Tsujimoto, D.-C. Nguyen, K. Manabe, and H. Nishino, "Doping effects in  $\text{Sb}_2\text{S}_3$  absorber for full-inorganic printed solar cells with 5.7% conversion efficiency," *Int. J. Hydrogen Energy*, accepted, in-press. DOI: 10.1016/j.ijhydene.2013.02.069.
- [37] K. Y. Rajpure and C. H. Bhosale, "(Photo)electrochemical investigations of spray deposited n- $\text{Sb}_2\text{S}_3$  thin film/polyiodide/C photoelectrochemical solar cells," *Mater. Chem. Phys.*, vol. 63, pp. 263–269, 2000.
- [38] R. Scheer, M. Wilhelm, H. J. Lewerenz, H. W. Schock, and L. Stolt, "Determination of charge carrier collecting regions in chalcopyrite heterojunction solar cells by electron-beam-induced current measurements," *Sol. Energy Mater. Sol. Cells*, vol. 49, pp. 299–309, 1997.

Authors' photographs and biographies not available at the time of publication.